Research Square

Preprints are preliminary reports that have not undergone peer review.
They should not be considered conclusive, used to inform clinical practice,
or referenced by the media as validated information.

Land use transitions and their impacts on carbon storage in the Yellow River Basin under different scenarios

Ruyang Xi
Shanxi Agricultural University
Ruiying Li
Shanxi Agricultural University
Jingxuan Wu
Shanxi Agricultural University
Fanyu Yue
Shanxi Agricultural University
Jiakai Ma
Shanxi Agricultural University
Zhilei Zhen
Shanxi Agricultural University
Ben Wang
wangben@sxau.edu.cn
Shanxi Agricultural University

Article

Keywords: land use change, carbon storage, PLUS-InVEST model, multi-scenario simulation, the Yellow River Basin

Posted Date: November 18th, 2026

DOI: https://doi.org/10.21203/rs.3.rs-11537295/v1

License: This work is licensed under a Creative Commons Attribution 4.0 International License.
Read Full License

Additional Declarations: No competing interests reported.

Land use transitions and their impacts on carbon storage in the Yellow River Basin under different scenarios

Ruyang Xi[1], Ruiying Li[2], Jingxuan Wu[2], Fanyu Yue[1], Jiakai Ma[2], Zhilei Zhen[2], Ben Wang[2]*

[1]College of Horticulture, Shanxi Agricultural University, Taigu, 030800, China

[2]College of urban and rural construction, Shanxi Agricultural University, Taigu, Shanxi 030800, China

Word Count: 7700 words (main body) with 11 figures and 7 tables

Article submitted to: Carbon Balance and Management

***Corresponding author**: Ben Wang* (wangben@sxau.edu.cn)College of forestry, Shanxi Agricultural University, Taigu, Shanxi 030801, China. **Tel.**: +8617835712255

Abstract: Terrestrial carbon sequestration capacity is closely tied to land use patterns, with different land cover types exerting distinct effects on carbon pools. Strategic optimization of land use configurations offers a viable pathway to enhance ecosystem carbon storage (CS). This study focuses on three representative Yellow River Basin (YRB) segments, namely the Shanxi (Shanxi section of the Yellow River Basin, SYRB), Gansu (Gansu section of the Yellow River Basin, GYRB), and Shandong (Shandong section of the Yellow River Basin, SDYRB) sections, using an integrated PLUS-InVEST approach with dynamic carbon density estimation to evaluate land use effects on CS from 2005 to 2023 and project 2035 trajectories under alternative scenarios. Results reveal: (1) CS increased by 0.85% in SYRB and 0.91% in GYRB from 2005 to 2023, while declining by 4.55% in SDYRB due to construction land expansion; changes in grassland and forest land (FL) were the primary drivers. (2) Multi-scenario 2035 simulations show divergent optimal pathways: SYRB peaks under Urban Organic Renewal Scenario (UORS) (1.277×10^9 t) and Territorial Spatial Planning Scenario (TSPS) (1.276×10^9 t); GYRB under TSPS (2.379×10^9 t), with Ecological Protection Scenario (EPS) lowest (2.343×10^9 t); SDYRB under TSPS (0.99×10^9 t), EPS worst (0.944×10^9 t). Thus, differentiated policies are needed: SYRB requires coordinated urban renewal and spatial planning; GYRB needs TSPS-oriented grassland management and unused land restoration; SDYRB should adopt TSPS to balance urbanization and cultivated land (CL) protection. (3) Driving mechanisms differ regionally: SYRB's CL-to-forest gains are partially offset by energy development; GYRB faces precipitation decline and overgrazing, requiring ecological migration and grassland restoration; SDYRB must reconcile urbanization with agricultural intensification via a CL-wetland system and improved compensation. We recommend differentiated "Three Zones and Three Lines" spatial controls, with SDYRB strictly protecting CL, GYRB restoring unused land, and SYRB coordinating forest conversion with new energy development, to jointly enhance YRB carbon sink function. This study provides theoretical support for ecological conservation in the Yellow River Basin.

Keywords: land use change; carbon storage; PLUS-InVEST model; multi-scenario simulation; the Yellow River Basin

1. Introduction

Global climate change has brought land use and land cover change (LUCC) to the forefront as a primary anthropogenic driver influencing carbon dynamics in terrestrial systems, representing a critical nexus where human activities and the environment interact [1, 2, 3]. Terrestrial ecosystems function as major reservoirs of global carbon, offering a relatively stable and secure mechanism for carbon sequestration that is indispensable for modulating the global climate [4, 5, 6]. CS, which is defined as the total quantity of carbon held within a given pool, serves as a key metric within the framework of ecosystem service evaluation and acts as a sensitive indicator of ecosystem productivity and its resilience to environmental disturbances [7, 8]. The YRB, serving as a national ecological security barrier and a core strategic zone for high-quality development, exhibits land use change impacts on carbon sink functions that are pivotal to achieving the "dual carbon" targets; the carbon sink function of its ecosystems holds substantial significance for realizing carbon neutrality [9, 10, 11, 12].

Despite its significance, a comparative analysis of the distinct characteristics across various segments of the YRB remains an underexplored area. For instance, the Shanxi portion is situated within the central Loess Plateau, a region of significant soil erosion; the Gansu segment occupies the environmentally vulnerable upper reaches; and the Shandong section lies in the lower reaches, a zone marked by high levels of economic activity, intensive agricultural practices, and rapid urbanization.The ecological functions of these three provincial sections differ markedly, necessitating targeted

comparative analysis [13, 14, 15, 16]. The significant differences in physiographic conditions, development stages, and policy orientations among these three sections have led to highly pronounced spatial differentiation in land use change trajectories and CS response mechanisms. Existing studies have largely focused on individual provinces or the entire basin scale. For instance, Fu et al. (2024) identified the conversion of bare land and grassland to FL as the primary cause of CS increase in the Ili-Tianshan region [17]. Research by Zhang Yan et al. (2024) on the Chengdu urban agglomeration indicated that a 7.5% decrease in CL and a 12.3% increase in construction land from 2000 to 2020 resulted in an 8.2% decline in CS, with multi-scenario simulations demonstrating that the Ecological Protection Scenario (EPS) could effectively mitigate carbon loss [18]. Additional research has projected future CS change trends in the Yiluo River Basin of Henan Province [19]. However, these studies are often confined to single provinces or specific tributaries, and there is a lack of systematic comparative research encompassing the upper, middle, and lower reaches of the basin. Furthermore, future scenario simulations often fail to sufficiently incorporate the differentiated territorial spatial strategies and policy orientations of each section, making it difficult to thoroughly elucidate the highly spatially differentiated mechanisms of basin-wide CS responses to land use change and to formulate precise, region-specific management strategies.

The quantitative evaluation of how LUCC affects CS is currently hampered by several methodological constraints. Conventional modeling approaches, including CA-Markov and CLUE-S, often fall short in their ability to effectively incorporate policy interventions and the intricacies of spatial competition among different land uses, which consequently undermines their utility for robust multi-scenario decision support. Furthermore, dynamic CS assessments predominantly rely on static land use data, thereby neglecting the cascading carbon effects induced by land use transitions. The PLUS model, employing the Land Expansion Analysis Strategy (LEAS) and the Cellular Automata based on multi-type Random Seeds (CARS) algorithm, can accurately quantify the contributions of diverse driving factors (e.g., physiographic conditions, socio-economic variables, and policy constraints) to land use change and generate high-precision multi-scenario land use maps based on a decision tree approach [20, 21]. The InVEST model, characterized by its flexible parameter adjustment, robust visualization capabilities, and cost-effectiveness, is widely employed for the quantitative assessment of ecosystem CS. Specifically, the InVEST CS and Sequestration module enables the quantitative retrieval of the spatiotemporal dynamics of ecosystem carbon pools through a “land use type–carbon density” transfer mechanism [22, 23]. The synergistic application of these two models provides methodological support for a comprehensive “land use change driver – spatial pattern evolution – CS response” chain analysis. For instance, Wu et al. (2024) analyzed the spatiotemporal evolution of multi-scenario land use and CS in Dalian City based on the PLUS-InVEST coupled model, indicating that the expansion of FL under the EPS is pivotal for enhancing CS, whereas the conversion of high-carbon-density land to construction land due to urban expansion constitutes the primary pathway of carbon loss [24]. Ji et al. (2025) used OPGD and MGWR models and found that slope and population density dominate CS spatial differentiation in Beijing-Tianjin-Hebei, with their interaction having the strongest explanatory power, and further revealed spatially heterogeneous effects via MGWR [25]. Although the aforementioned studies have achieved significant progress in scenario construction and mechanism analysis, most remain insufficient in the differentiated scenario setting and systematic comparison tailored to characteristic territorial spatial strategies. In this context, this study focuses on the typical provincial sections of the YRB and introduces a regionally adapted multi-scenario framework, aiming to deepen the understanding of the basin-wide spatial differentiation mechanism of CS and to provide a scientific basis for precise ecological management.

This study takes the Shanxi-Gansu-Shandong section (SGS) of the YRB as the study area. It aims to systematically analyze the spatiotemporal differentiation characteristics of land use transition in this region from 2005 to 2023, simulate the evolutionary trends of the land use pattern in 2035 under four different scenarios—the Natural Development Scenario (NDS), Urban Organic Renewal Scenario (UORS), Territorial Spatial Planning Scenario (TSPS), and EPS—and evaluate the differential impacts of these various scenarios on the spatial distribution and total magnitude change of ecosystem CS. The research findings will provide a scientific basis for enhancing basin-scale carbon sink potential, promoting intensive land use, and facilitating regional synergistic governance, thereby supporting

the implementation of the national strategy for ecological conservation and high-quality development in the YRB.

2. Research Methods and Data Sources

2.1. Study area

The YRB traverses China's three major geographic gradients from west to east, resulting in pronounced differences in the natural environment and socio-economic development among its upper, middle, and lower reaches. This study selects the GYRB, SYRB, and SDYRB within the SGS Corridor of the YRB as typical regions for comparative analysis (Fig. 1).

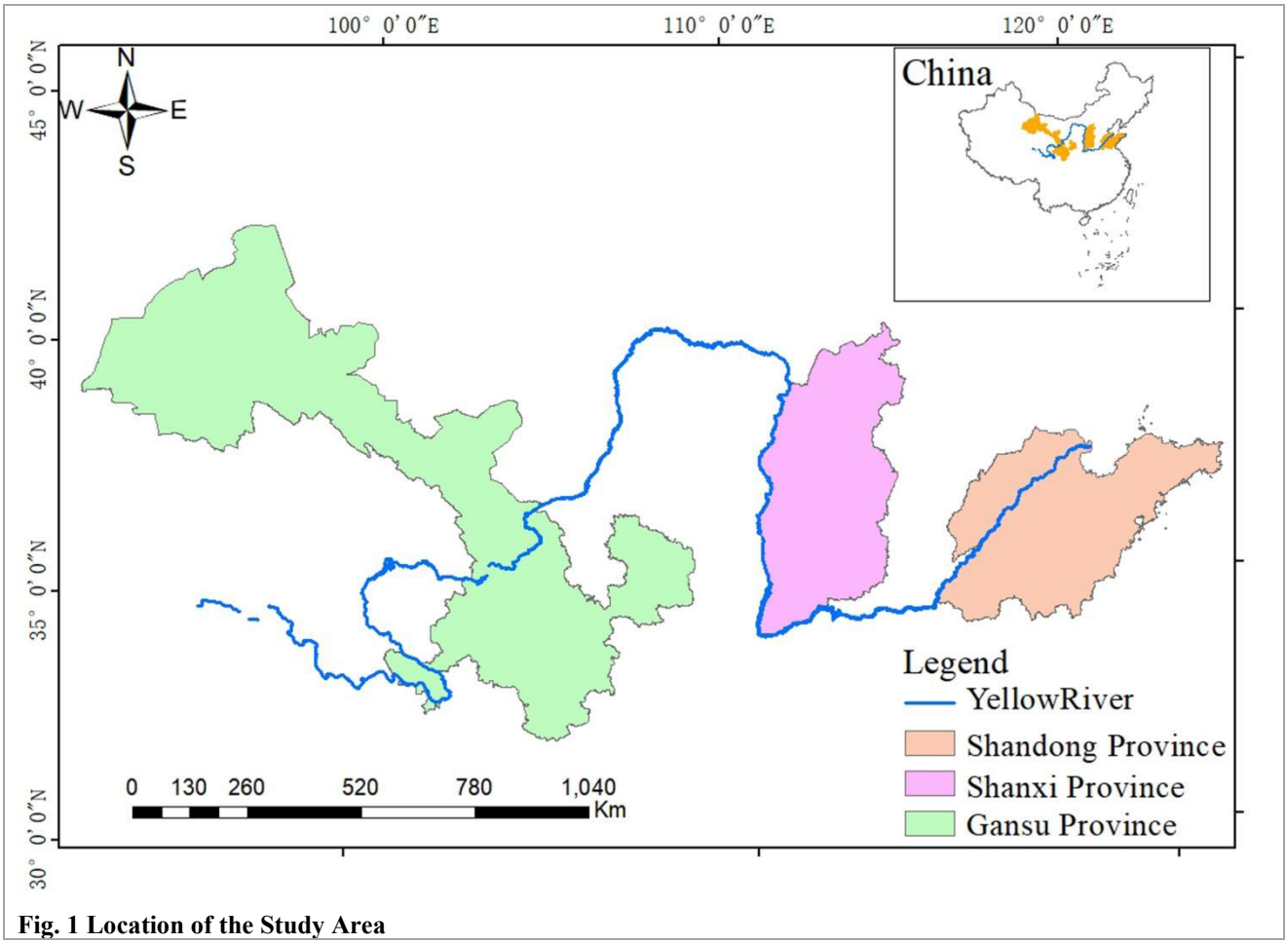


Fig. 1 Location of the Study Area

The study area designated as SYRB is geographically positioned between 110°14′–114°33′E and 34°34′–40°31′N. It encompasses three principal geomorphological features: the Shanxi Plateau, the Taiyuan Basin, and the Yuncheng Basin, stretching from Pianguan County in the north to Yuanqu County in the south (Fig. 2a). Climatically, this region falls under the temperate continental zone, receiving an average annual precipitation of 508.8 mm and maintaining a mean annual temperature of 8°C. A critical function of this area is its role as a key zone for water resource conservation and aquifer recharge in northern China. Furthermore, this region constitutes an integral component of Shanxi Province's new urban-rural regional development layout of "One Group, Two Zones, and Three Circles" , and is typical and representative for studying the social, economic, and ecological dimensions of urban development.

The SDYRB (114°47′–122°43′E, 34°22′–38°24′N) primarily encompasses three geomorphological units: the central-southern low-mountain and hilly region of Shandong, the Jiaolai Plain region, and the northwestern Shandong Yellow River floodplain region, extending from Heze City in southwestern Shandong to Weihai City at the easternmost tip of the Jiaodong Peninsula (Fig. 2b). The total terrestrial area of the region is approximately 158,000 km², including 16 prefecture-level cities with subordinate districts and 136 county-level administrative units, accounting for 1.6% of China's total terrestrial area. The study area is the core zone of the Shandong Peninsula Urban Agglomeration, holding a crucial position in the national strategies for ecological conservation and high-quality development in the YRB and the maritime power strategy, and exhibits a high degree of representativeness in terms of population, economy,

agriculture, and marine resources.

The GYRB (92°13′–108°46′E, 32°31′–42°57′N) traverses three major geomorphological units: the Hexi Corridor Plain region, the central Gansu Loess Plateau region, and the southern Gansu mountainous region, extending from Dunhuang City at the western end of the Hexi Corridor to Wenxian County at the southernmost tip of Longnan (Fig. 2c). The climate types in this region are complex and diverse, predominantly temperate continental climate and plateau mountain climate, with a mean annual precipitation of approximately 300 mm and a mean annual temperature of approximately 8°C. The GYRB serves as a vital ecological barrier, an energy base, and a key node along the land route of the "Belt and Road" initiative in northwestern China. The study area is a pivotal hub connecting the Central Plains, Northwest China, and the Qinghai-Tibet Plateau, playing a crucial role in the national strategies for the large-scale development of western China, ecological conservation and high-quality development in the YRB, and the "Belt and Road" construction, and is markedly representative in terms of ecological diversity, energy resources, and ethnic culture.

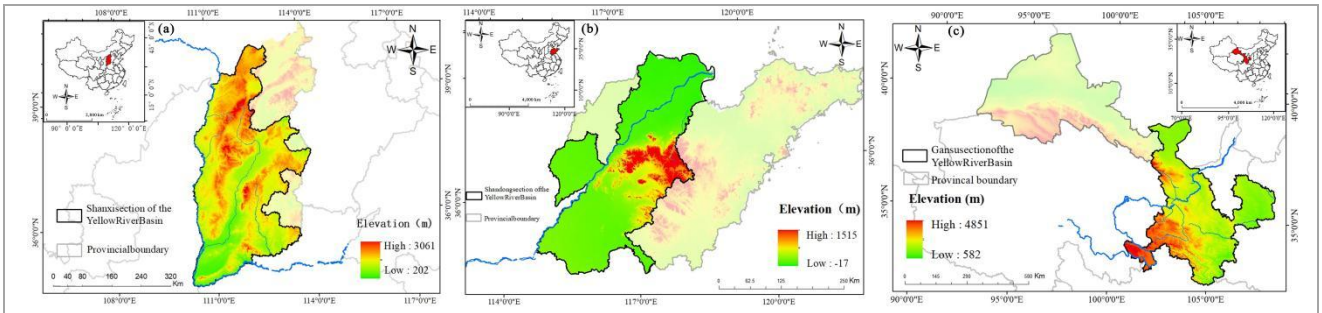


Fig. 2 Spatial characteristics of the SYRB, SDYRB, and GYRB

2.2. Data Sources and Processing

2.2.1 Data Sources

Land use data sources: Land use classification was extracted from Landsat imagery (2005–2023) using support vector machine classification, with an overall accuracy exceeding 85%, covering the three provincial sections. The classification system includes CL, FL, grassland, water bodies, construction land, and unused land (Table 1). These driving factors are categorized into natural factors (elevation, slope, precipitation), socio-economic factors (GDP, population density, road network), and policy factors (Grain for Green project areas, CL conservation zone boundaries). The spatial distributions of the selected driving factors for the SYRB, GYRB, and SDYRB are shown in Figures 3, 4, and 5, respectively. These factors exhibit distinct spatial heterogeneity.

Table 1 Data Sources

Data Type	Data	Data Source
Land Use Data	Annual China Land Cover Dataset	https://essd.copernicus.org/articles/13/3907/2021/
Socio-economic Data	Population Count	https://hub.worldpop.org/geodata/listing?id=77
	Gross Domestic Product	https://www.resdc.cn/DOI/doi.aspx?DOIid=33&WebShieldSessionVerify=Hj9ajWuOmMQM4del0wVT
	Vector Road Network Data	https://www.openstreetmap.org
Climate and Environmental Data	Mean Annual Precipitati	https://doi.org/10.5281/zenodo.3185722

on Dataset	
Mean Annual Temperature Dataset	https://doi.org/10.11888/Meteoro.tpdc.270961
Slope Data	https://www.gscloud.cn/search
Terrestrial Ecosystem Carbon Density Dataset of China (2010s)	http://www.nesdc.org.cn/sdo/detail?id=5fa53685042ebb70d0c8340b

2.3 Model Methods

2.3.1 InVEST Model

We used the InVEST model's Carbon module to estimate carbon storage (CS) from land use data across four pools: aboveground biomass, belowground root biomass, soil organic carbon, and dead organic matter. For each land use type, total CS was the sum of pool carbon densities multiplied by its area, and regional CS was the sum over all types. Land use data were obtained from the Chinese Academy of Sciences, while carbon density baselines for the three sections came from the National Ecosystem Science Data Center's 2010s dataset, supplemented by prior studies. To correct for spatial-temporal variations, we computed adjustment coefficients from ratios of local to national mean annual precipitation and temperature, following the empirical relationships [26, 27, 28]. Biomass correction used both precipitation- and temperature-based coefficients, whereas soil correction used only precipitation. The corrected densities for each land use in SYRB, GYRB, and SDYRB are given in Tables 2–4.

Table 2 Corrected values of ecosystem carbon density for the SYRB t·hm^{-2}

Land Use Type	Aboveground Carbon Density	Belowground Carbon Density	Soil Carbon Density	Dead Organic Matter Carbon Density
CL	3.90	29.54	69.70	1.20
FL	16.70	39.50	98.78	2.51
Grassland	8.90	20.22	63.69	1.10
Water	0.70	0	0	0
Unused Land	0.69	0.12	18.42	0
Construction Land (COL)	1.84	9.37	0.85	0

Table 3 Corrected values of ecosystem carbon density for the GYRB t·hm^{-2}

Land Use Type	Aboveground Carbon Density	Belowground Carbon Density	Soil Carbon Density	Dead Organic Matter Carbon Density
CL	3.21	15.45	91.85	1.85
FL	8.19	22.14	134.19	2.62
Grassland	6.56	16.32	84.09	1.43
Water	0.08	0	0	0
Unused Land	0.25	0.07	19.10	0
COL	0.48	5.47	0.81	0

Table 4 Corrected values of ecosystem carbon density for the SDYRB t·hm^{-2}

Land Use Type	Aboveground Carbon Density	Belowground Carbon Density	Soil Carbon Density	Dead Organic Matter Carbon Density
CL	19.72	33.31	108.02	1.63

FL	36.70	46.36	127.79	4.27
Grassland	13.19	35.57	98.90	0.62
Water	0.66	0	13.47	0
Unused Land	2.05	0.55	22.49	0
COL	4.03	0.37	1.02	0

154

155 2.3.2 PLUS Model

156 Developed by the China University of Geosciences from the FLUS model, the PLUS model is a grid-based
157 patch-generating land use change prediction model. It couples the LEAS (Land Expansion Analysis Strategy)
158 simulation framework with a CA model (Cellular Automata based on Multiple Random Seeds, CARS) [29], and offers
159 advantages for dynamically simulating land use patch changes [30]. By integrating and analyzing two-period land use
160 data, the model can identify change drivers, simulate patch-level transitions across multiple land types, and assist
161 regional planning policies in achieving sustainable development. Future land use demand and dynamics under multiple
162 scenarios are simulated by setting transition and development probabilities for different scenarios using the PLUS
163 model.

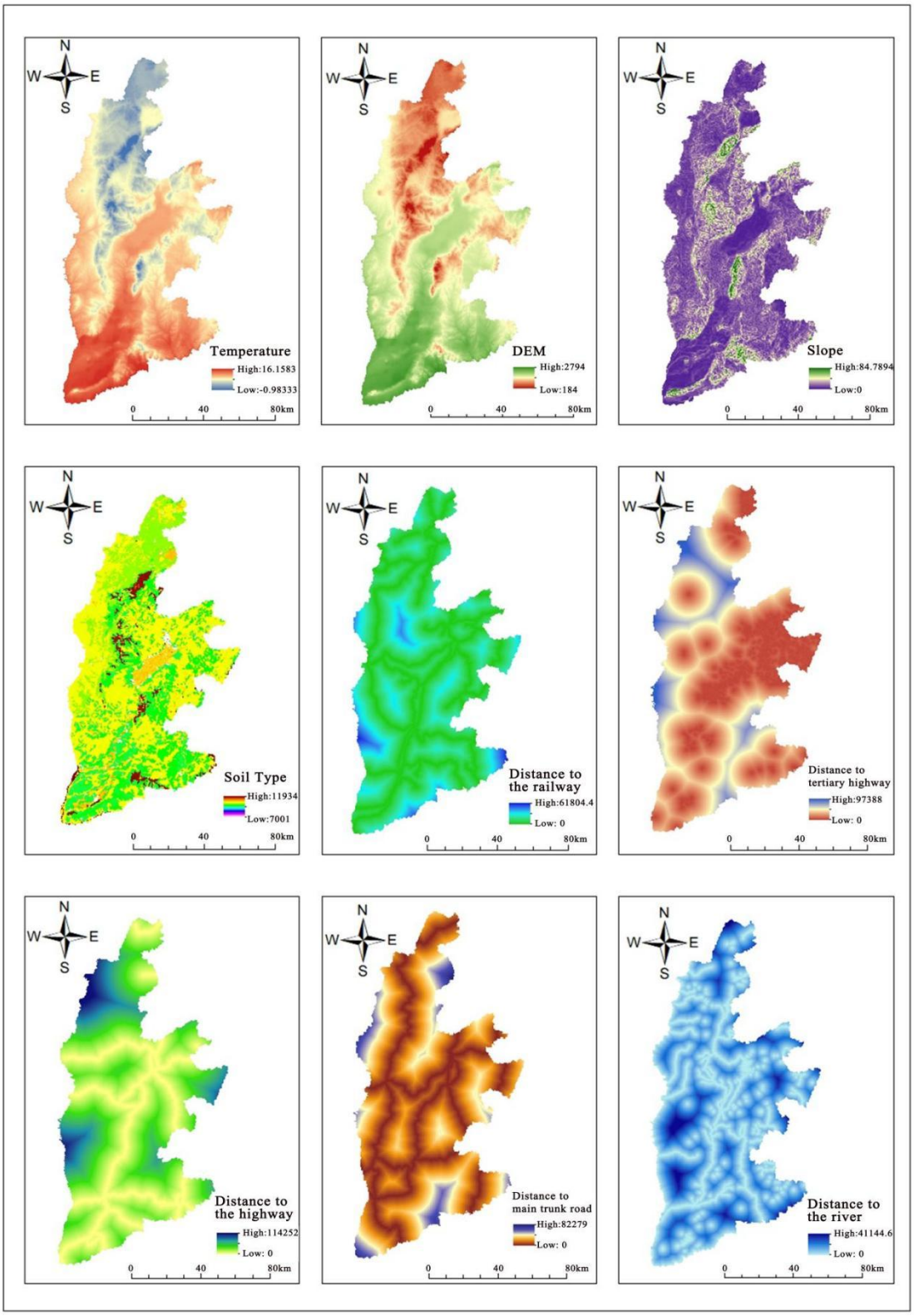


Fig. 3 Spatial distribution of driving factors for land use simulation in the SYRB

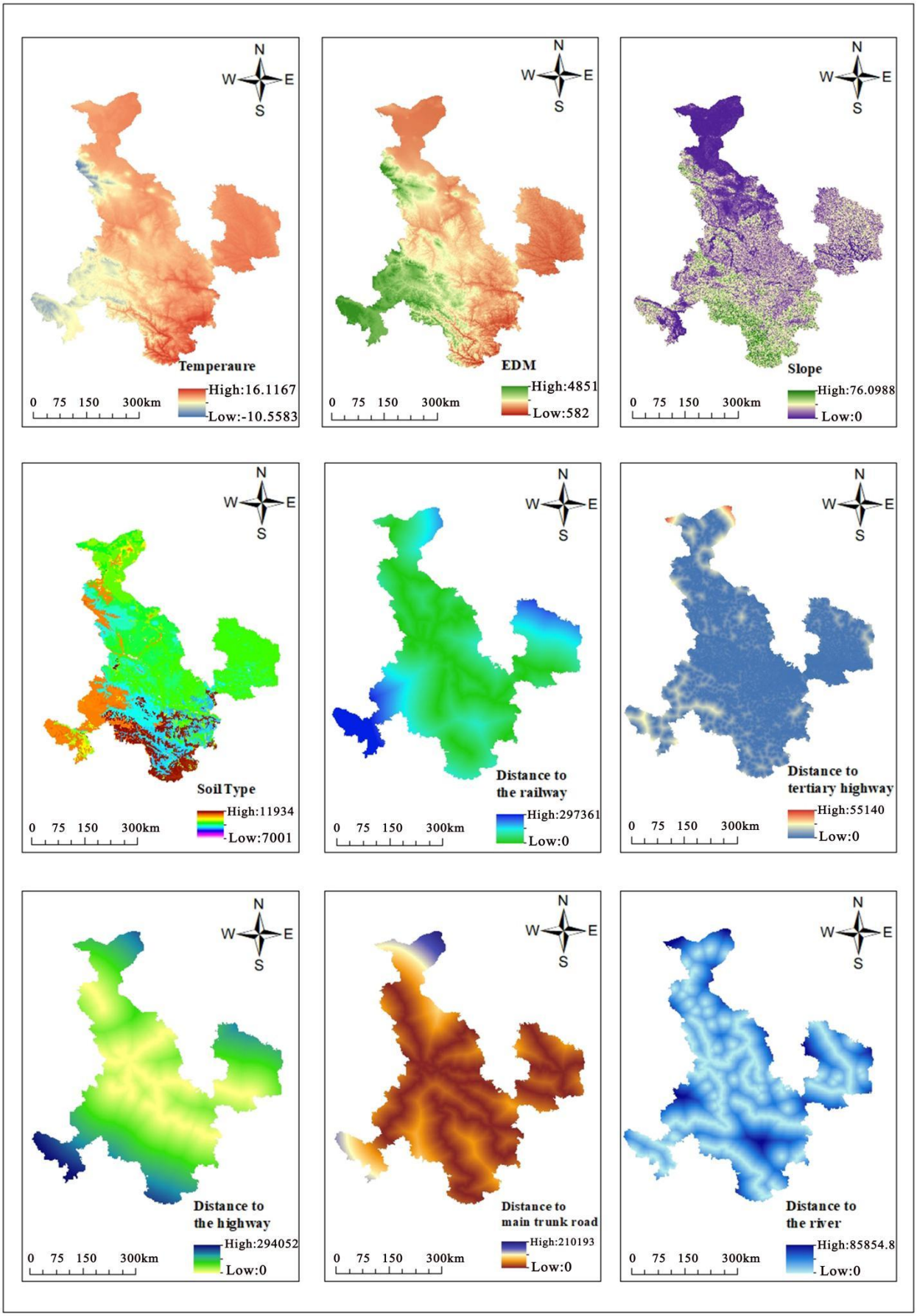


Fig. 4 Spatial distribution of driving factors for land use simulation in the GYRB

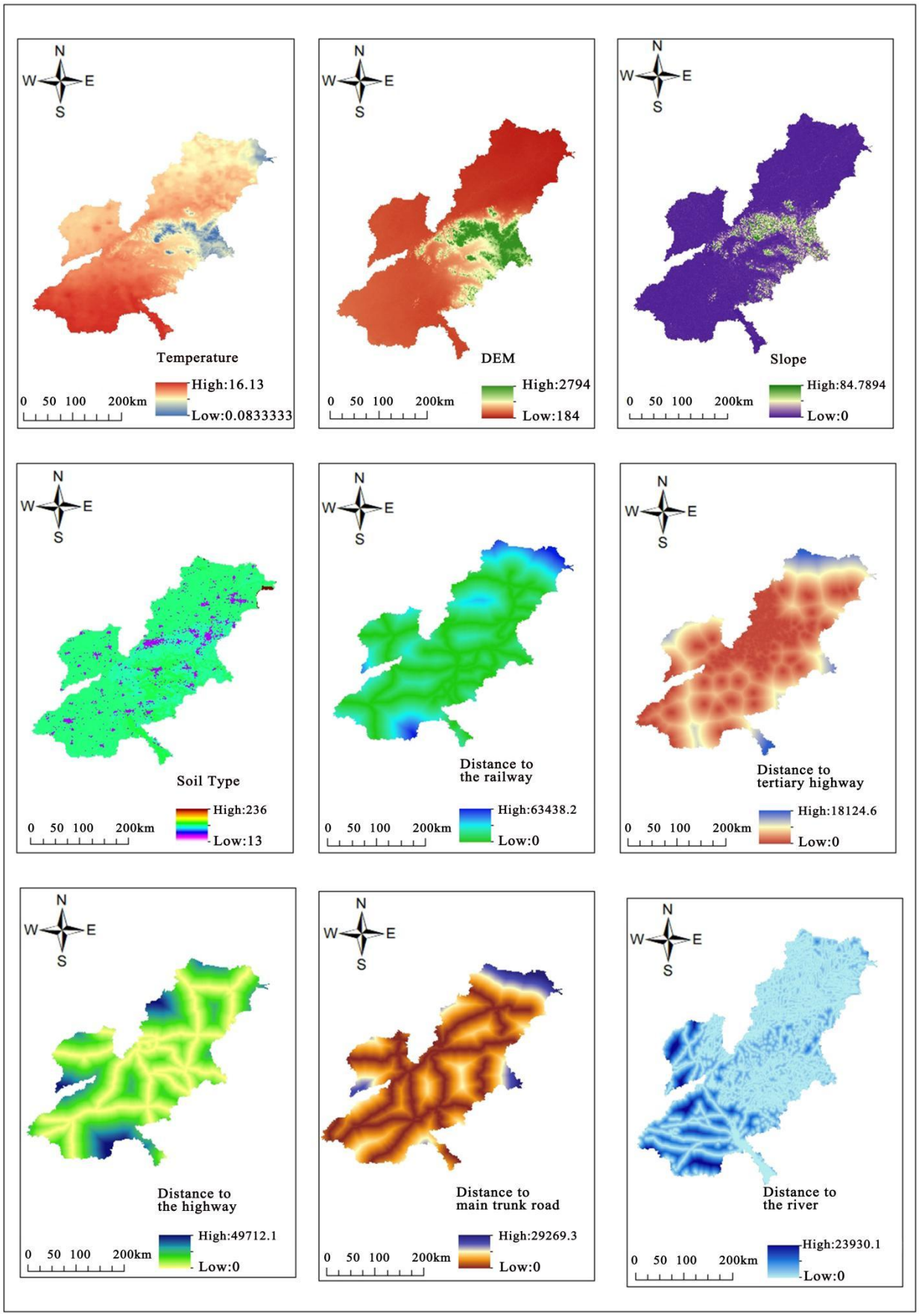


Fig. 5 Spatial distribution of driving factors for land use simulation in the SDYRB

2.3.3 Scenario Setting

In simulating future land use pattern scenarios, four scenarios—Natural Development, Urban Organic Renewal, Territorial Spatial Planning, and Ecological Protection—were established with reference to the Plan for Ecological Conservation and High-quality Development in the YRB, the Plans for Ecological Conservation and High-quality Development in the YRB for Shanxi/Gansu/Shandong Provinces, and the Territorial Spatial Plans of Shanxi, Gansu, and Shandong Provinces (2021–2035).

2.3.4 Accuracy Verification

Land use distributions for the SGS Corridor in 2035 were simulated using the PLUS model, with 2005 and 2023 data as the baseline and the LEAS and CARS modules integrated. Model validation was performed by comparing the simulated 2035 land use data against actual observations through PLUS's validation module. The procedure involved four steps: (1) extracting land use expansion from 2005 to 2023 by converting data to PLUS input format; (2) generating land use development potential and calculating 2035 land use demand via the Markov chain; (3) producing simulated land use distributions for the SYRB, SDYRB, and GYRB in 2035 based on Markov chain predictions; and (4) computing the Kappa coefficient using confusion matrix and Figure of Merit (FOM) validation tools [31, 32]. The model achieved an overall reliability score of 0.90 and a Kappa coefficient of 0.85, confirming its high predictive accuracy for future land use types. Accordingly, the PLUS model was employed to simulate the 2035 land use patterns of the SGS Corridor, with transition rules detailed in Table 5.

Table 5 Multi-scenario transition matrix settings

Land Use Type	Natural Development Scenario						Urban Organic Renewal Scenario						Territorial Spatial Planning Scenario						Ecological Protection Scenario					
	CL	**FL**	**GL**	**WA**	**COL**	**UL**	**CL**	**FL**	**GL**	**WA**	**COL**	**UL**	**CL**	**FL**	**GL**	**WA**	**COL**	**UL**	**CL**	**FL**	**GL**	**WA**	**COL**	**UL**
CL	1	1	1	0	1	1	1	1	1	0	0	0	1	1	1	0	0	0	1	1	1	1	1	1
FL	1	1	1	0	0	1	0	1	1	1	0	0	0	1	1	0	0	0	0	1	0	0	0	0
Grassland	1	1	1	1	1	1	0	1	1	1	0	0	0	1	1	0	0	0	0	1	1	1	0	0
Water	0	1	1	1	0	0	0	0	0	1	0	0	1	1	1	1	1	0	0	0	0	1	0	0
COL	0	0	0	0	1	0	1	1	1	0	1	0	0	0	0	0	1	0	0	0	0	0	1	0
Unused Land	1	1	1	1	1	1	1	1	1	1	1	1	1	1	1	1	1	1	1	1	1	1	1	1

3. Results and Analysis

3.1 Land Use Change (2005–2023)

3.1.1 Land Use Change in the SYRB from 2005 to 2023

Within the SYRB, CL and grassland constituted the predominant land cover categories, with forestland ranking third. A descending order of total area was observed as follows: CL > grassland > forestland > construction land > water bodies > unused land. Throughout the 18-year study interval, the most substantial transformations were recorded for CL, grassland, and forestland. Fig. 6 illustrates the land use transfer dynamics.

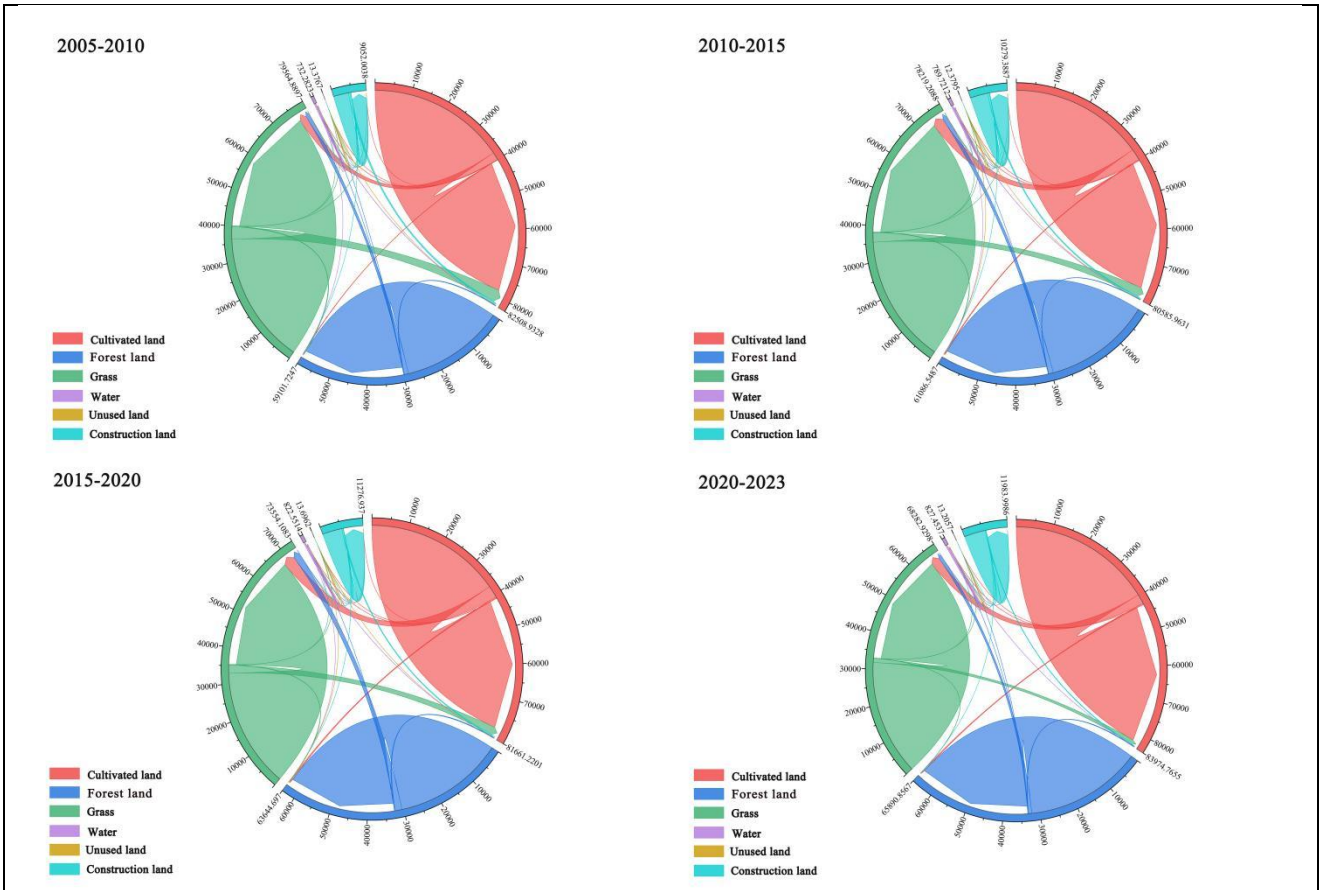


Fig. 6 Chord diagram of the land use transfer matrix for the SYRB from 2005 to 2023

From 2005 to 2010, CL experienced a pronounced decline, with its area proportion decreasing from 36.64% to 34.97% of the total regional area—a net reduction of 1.67 percentage points (approximately 1,909 km²). From 2015 to 2020, the proportion of CL continued to decline, though at a more moderate pace, decreasing from 35.74% to 34.99% (a net loss of 0.75 percentage points, approximately 863 km²). Among these, construction land exhibited the largest increase, expanding by 476.10 km², accounting for 5.40% of the total newly added area. In contrast, the changes in water bodies and unused land were relatively minor, decreasing by 42.55 km² and 3.84 km², respectively. From 2010 to 2015, 241.49 km² of FL and 25.55 km² of water bodies were converted to CL, while only 6.64 km² of FL was converted to construction land. Between 2020 and 2023, mutual conversions among CL, FL, and grassland were significant, with substantial area changes. The area of grassland converted to CL was 2,642.71 km², that of FL converted to CL was 307.03 km², while the areas of CL converted to FL and grassland were 184.09 km² and 1,141.53 km², respectively, and the area of CL converted to construction land was 203.75 km². The area of land used for construction expanded to 6,120.09 km², directly reflecting the considerable scale of land development in Shanxi in recent years.

3.1.2 Land Use Change in the GYRB from 2005 to 2023

The land use types in the GYRB are dominated by grassland and CL, followed by FL. The most notable dynamic changes during the study period were observed in CL, grassland, and FL. Fig. 7 illustrates the land use transfer dynamics. Over the past 18 years, land use change has exhibited the core characteristics of "CL shrinkage, FL expansion, and grassland fluctuation." Specifically, the CL area continuously decreased by 6,183.48 km², FL expanded by 5,226.28 km², while the change in grassland stabilized, fluctuating within a range of 245.80 km².

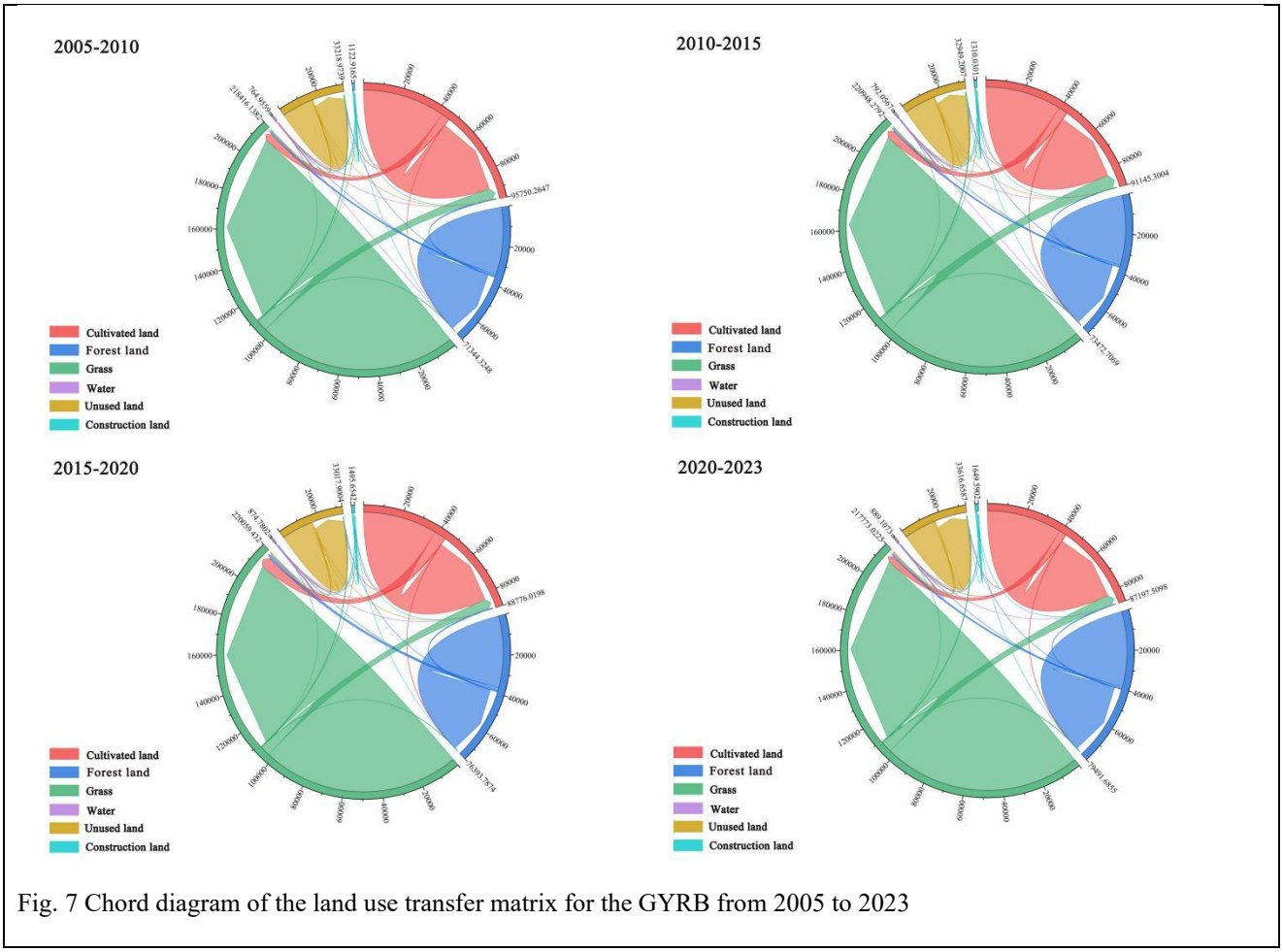


Fig. 7 Chord diagram of the land use transfer matrix for the GYRB from 2005 to 2023

From 2005 to 2010, the CL area decreased sharply, with a net reduction of 1,879.29 km², primarily converted to grassland, which accounted for 90.26% of the total CL loss. From 2010 to 2015, significant grassland area loss was evident, with 4,636.88 km² and 1,030.51 km² converted to CL and FL, respectively, and 525.60 km² converted to unused land, exacerbating local land desertification. From 2015 to 2020, the proportion of grassland fluctuated slightly from 53.02% to 51.62%. Notably, water bodies, unused land, and construction land all increased, with unused land exhibiting the largest increase, expanding by 790.31 km² by 2020; the changes in water bodies and grassland were relatively modest, increasing by 104.20 km² and 107.27 km², respectively. During the 2020–2023 period, mutual conversions among CL, FL, and grassland continued. Nearly 94.88% of the newly added CL area was derived from grassland conversion, the area of grassland converted to FL reached 1,053.35 km², and the area of CL converted to grassland was 5,330.14 km². In contrast, the area converted to construction land was only 25.48 km², which was less than 1% of the total CL area in 2020. The land used for construction remained almost unchanged compared to 2020, with only 0.7551 km² of land converted to water bodies.

3.1.3 Land Use Change in the SDYRB from 2005 to 2023

Land use change in the SDYRB exhibits distinct characteristics of "CL dominance and ecological optimization," with the main land use types being CL, grassland, and FL. From 2005 to 2023, the CL area continuously decreased from 53,478.06 km² to 48,305.57 km², with total reduction of 9.67% over the 18-year study period (approximately 0.56% per year). Meanwhile, construction land expanded from 11,278.01 km² to 16,498.12 km², an increase of 46.28%, highlighting the rapid urbanization process (Fig. 8).



Fig. 8 Chord diagram of the land use transfer matrix for the SDYRB from 2005 to 2023

From 2005 to 2010, CL decreased by 1,679.09 km², primarily converted to construction land, which accounted for 68.91% of the total CL loss. From 2010 to 2015, the water area achieved a breakthrough, with the total water area reaching 2,854.30 km² by 2015, mainly derived from the conversion of 280.31 km² of unused land, reflecting the effectiveness of the wetland restoration project at the Yellow River Estuary. CL continued to decrease, but the structure of its conversion shifted toward construction land and water bodies. By 2020, the proportion of construction land had reached 21.93% of the total land area. Notably, both water bodies and FL increased during the 2015–2020 period, expanding by 689.90 km² and 309.24 km², respectively, while the change in unused land was the smallest, increasing by only 32.53 km². During the 2020–2023 period, the proportions of CL, FL, and grassland gradually stabilized.

3.2 Land Use Change under Different Scenarios in 2035

Based on the PLUS model and the existing land use statistical data from 2005 to 2023, this study projected the land use changes in the eastern, central, and western sections of the YRB—the SGS Corridor—under four different scenarios for 2035, as illustrated in Fig. 9.

Under the NDS, construction land in the SYRB will continue to expand and is projected to encroach upon 1,723.58 km² of CL, primarily concentrated in the Taiyuan-Jinzhong metropolitan area (red patch area). This trend exhibits path dependence on the historical trajectory observed from 2005 to 2023. Under the EPS, through mandatory constraints, 1,250.35 km² of newly added FL can be achieved in the Lüliang Mountain area, representing an increase of 3.88% compared to 2023, albeit at the cost of a 2.15% reduction in CL. The TSPS indicates that the growth of construction land in the Taiyuan-Xinzhou Economic Zone will be controlled at 64.70% of the historical average, with 387.42 km² of CL supplemented through the reclamation of abandoned industrial and mining land (Fig. 9a).

Under the EPS for the GYRB, the desertification control efforts in the Hexi Corridor have yielded remarkable results, with the conversion rate of unused land reaching 18.35%, of which 14.72% was primarily converted to FL and grassland; however, the risk of grassland overloading remains. The UORS may trigger encroachment upon the Heihe

Wetland, with the proportion of construction land projected to increase by an overall 6.84%. Specifically, the construction land expansion in Zhangye City is projected to exceed the ecological redline by 12.75 km² (Fig. 9b).

Under the requirements of the TSPS for the SDYRB, the scale of sea reclamation in the Jiaodong Peninsula is compressed to an annual average of 9.83 km². Under the EPS, the restoration of the Yellow River Delta wetlands could expand the water area by 315.67 km², but would consequently reduce the construction land development intensity in Dongying City to 15.04%. Notably, the "non-grain" conversion rate of CL in the SDYRB exceeded 35% across all scenarios, which poses a threat to the bottom line of food security (Fig. 9c).

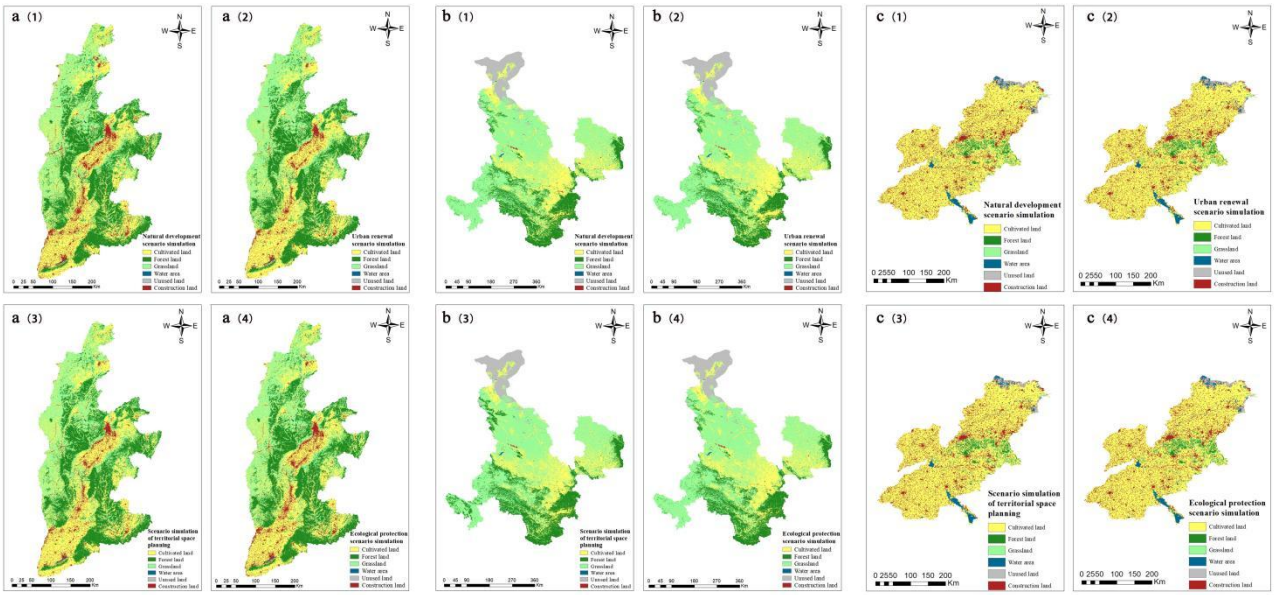


Fig. 9 Projected land use for the Shanxi, Gansu, and Shandong sections of the YRB under different scenarios in 2035

3.3 Characteristics of CS Change

3.3.1 Temporal Change in CS

Table 6 CS (t) of the SYRB, SDYRB, and GYRB from 2005 to 2023

Study Area	2005	2010	2015	2020	2023
SYRB	1,275,875,982	1,274,002,835	1,275,915,749	1,282,908,261	1,286,780,533
SDYRB	1,035,505,499	1,019,060,595	1,007,722,391	993,430,954	988,355,854
GYRB	2,348,030,638	2,353,175,884	2,358,914,252	2,366,002,040	2,369,438,665

Applying the InVEST model to the processed data revealed distinct temporal trends in CS for each of the three study sections between 2005 and 2023. Carbon stocks in the SYRB demonstrated a consistent upward trajectory, growing from 1.28 × 10^9 t to 1.29 × 10^9 t (a 0.85% increase), which points to a progressive strengthening of its carbon sink function. In stark contrast, the SDYRB experienced a persistent decline, with its CS falling from 1.04 × 10^9 t to 0.99 × 10^9 t (a 4.55% decrease), underscoring the detrimental effect of urban expansion on carbon retention capacity. The GYRB, like the SYRB, showed an increasing trend, with its total CS far exceeding that of the SYRB, rising from 2.35 × 10^9 t to 2.37 × 10^9 t, an increase of approximately 0.91%, reflecting the positive effects of ecological conservation measures (Table 6).

Table 7 Projected CS (t) under different scenarios for the SYRB, SDYRB, and GYRB in 2035

Study Area	NDS	UORS	TSPS	EPS

SYRB	1,261,061,740.32	1,277,257,675.51	1,275,992,920.48	1,264,401,565.53
SDYRB	945,429,360.26	982,187,034.44	989,649,744.13	944,489,144.45
GYRB	2,352,058,423.38	2,348,030,637.66	2,379,698,576.44	2,343,154,339.40

Multi-scenario projections of CS for 2035 revealed divergent optimal scenarios among the three provincial sections (Table 7). In SYRB, the highest CS was projected under UORS (1.28×10^9 t), closely followed by TSPS (1.28×10^9 t), representing increases of 16.2×10^6 t and 14.9×10^6 t relative to NDS, respectively. EPS yielded 1.26×10^9 t, a modest increase of 3.3×10^6 t over NDS but considerably lower than UORS and TSPS. In GYRB, TSPS achieved the highest CS (2.38×10^9 t), exceeding NDS by 27.6×10^6 t, while EPS resulted in the lowest value (2.34×10^9 t), 8.9×10^6 t lower than NDS, indicating that ecological protection alone cannot offset carbon losses from restricted land use conversions. In SDYRB, TSPS produced the highest CS (0.99×10^9 t), followed by UORS (0.98×10^9 t), with increases of 4.7% and 3.9% over NDS, respectively; EPS performed worst (0.94×10^9 t), slightly below NDS.

At present, inter-provincial differences exist in China's territorial spatial planning. Under the TSPS, the CS of the GYRB reaches 2.38×10^9 t, the highest value among the three sections, whereas SYRB under TSPS (1.276×10^9 t) is slightly lower than UORS (−0.04%) but still 1.2% higher than NDS, indicating that territorial spatial planning needs to be tailored to local conditions. These results indicate that TSPS and UORS generally outperformed EPS in preserving CS, while EPS provided limited benefits only in SYRB and led to carbon losses in GYRB and SDYRB.

The CS of the SYRB is the lowest among the three but relatively stable, standing at 1.28×10^9 t in 2005 and increasing slightly to 1.29×10^9 t in 2023, with a growth rate of 0.85%. Its northern mountainous areas exhibit good forest cover, with carbon density reaching up to 157.49 t/ha, forming a significant high-value CS zone. In contrast, the southern basins, influenced by CL and construction land, exhibit lower CS.

Multi-scenario projections for 2035 further highlighted spatial differentiation. Under EPS, the CS of the GYRB was projected to reach 2.34×10^9 t, a decrease of 2.6×10^7 t compared to 2023, indicating that the potential of unused land remediation had not been fully realized under a purely protection-oriented approach (Fig. 10b). In contrast, under TSPS, GYRB reached 2.38×10^9 t, the highest among all scenarios, demonstrating that integrated spatial planning is essential for enhancing carbon sinks in arid regions. The CS of the SDYRB varied considerably across scenarios, with TSPS yielding the highest value (0.99×10^9 t) and EPS the lowest (0.94×10^9 t) (Fig. 10c). The CS of the SYRB reached 1.28×10^9 t under both UORS and TSPS, whereas under EPS it was 1.26×10^9 t. The UORS exerted a positive effect on the SYRB through controlled urban densification and land consolidation; however, the low-density characteristic of construction land still partially suppressed CS growth (Fig. 10a). The high-value areas of the GYRB benefited from grassland and forest conservation, but the lowest CS under EPS suggested that restricting land use conversions without active restoration measures may exacerbate carbon losses. The declining trend of the SDYRB originated from the rapid conversion of CL to construction land, which weakened its carbon sink function, consistent with historical trends; TSPS offered the most effective pathway for mitigating this decline by curbing disorderly urban expansion and protecting ecological land. The stability of the SYRB's CS was attributable to the carbon sequestration effect of FL in the northern region; however, the potential for carbon sink growth in the southern region remained unrealized due to CL conservation policy constraints.

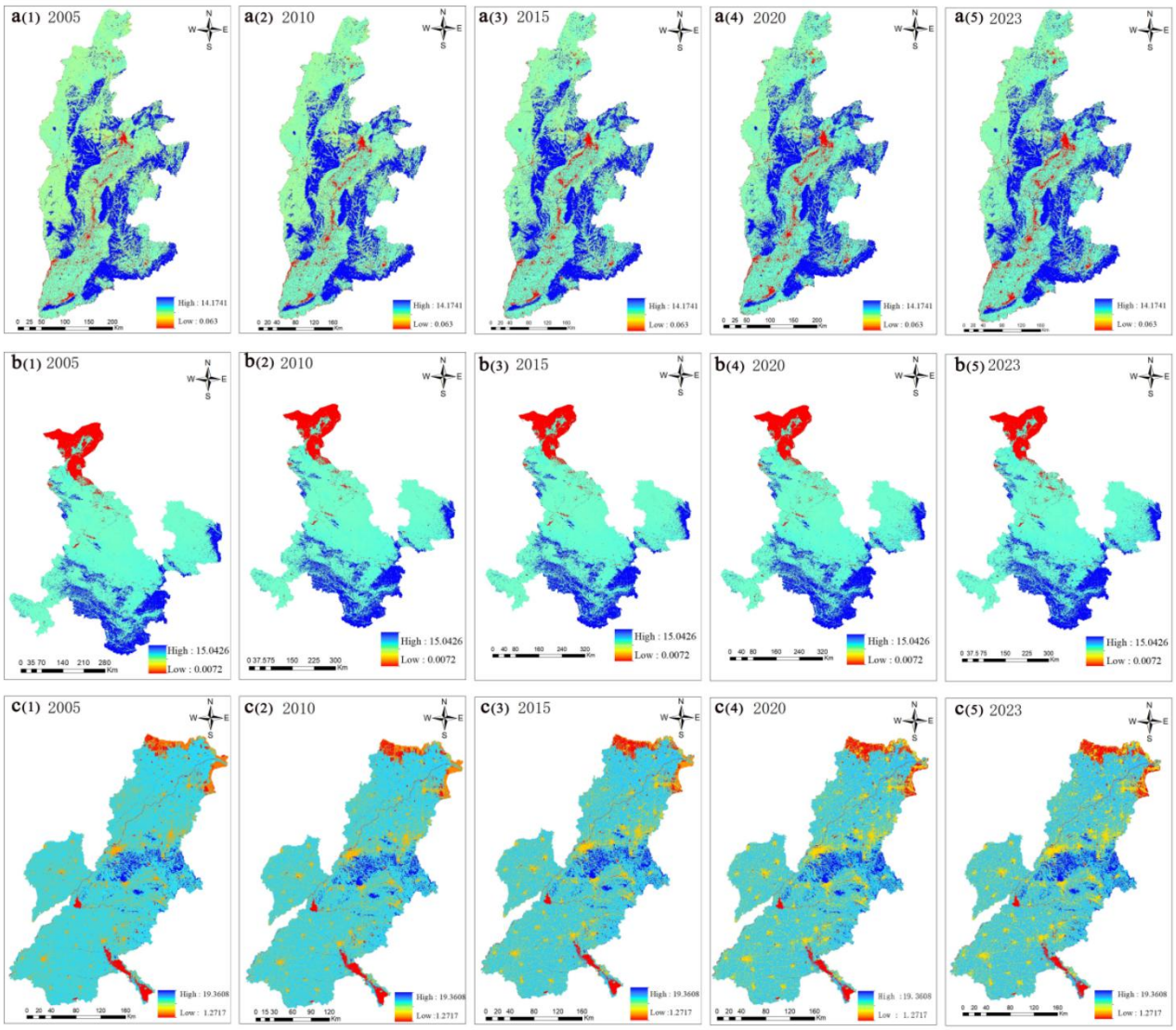


Fig. 10 Changes in CS in the Shanxi, Gansu, and Shandong sections of the YRB from 2005 to 2023

3.4 Impact of Land Use Change on CS

The CS of the SGS Corridor was analyzed based on the land use transfer matrix and carbon density values for different regions. The results indicate that changes in land use types have driven the overall variation in CS across the SGS Corridor. From 2005 to 2023, the total expansion of construction land across the three provincial sections amounted to 3,225 km², of which the SYRB accounted for 46.4%, primarily encroaching upon CL (54.7%) and FL (28.6%), thereby triggering the conversion of high-carbon-density land to low-carbon-density land and resulting in carbon loss.

The expansion of construction land in the SYRB was mainly concentrated in the Taiyuan Basin, with an expanded area of 1,580 km², causing a carbon loss of 1.16×10^7 t. From 2015 to 2023, the proportion of construction land rose from 1.44% to 2.44%, while the CS increased by only 0.9% during the same period, reaching 1.29×10^9 t. This suggests that energy development has, to a certain extent, offset the benefits of ecological restoration.

In the GYRB, construction land was predominantly distributed along the Hexi Corridor. The conversion of unused land to grassland increased the carbon sink by 7.71×10^7 t; however, overgrazing led to grassland degradation, with a degraded area of 2,560 km² and a carbon loss of 1.33×10^7 t, causing the CS to exhibit a U-shaped fluctuation.

In Shandong, construction land in the Jiaodong Peninsula exhibited a pattern of contiguous expansion, with the area of FL converted to construction land reaching 796 km². Concurrently, CL loss amounted to 22,172 km² between

2000 and 2020, leading to a continuous 4.55% decline in CS, which fell to 9.88 × 10^8 t in 2023.

Scenario simulations for 2035 based on the PLUS model clearly demonstrate that territorial spatial planning has become the "critical valve" determining the trajectory of CS. With planning as the pivot, the GYRB converted unused land in areas such as the Hexi Corridor entirely into a shrub-grass composite system, adding a new carbon sink of 7.71 × 10^7 t, propelling the provincial CS from 2.37 × 10^9 t in 2023 to first decline and then rise, ultimately reaching 2.38 × 10^9 t and achieving a net increase of 0.45%. Through the coupled implementation of the "Grain for Green Project and mine reclamation," the CS of the SYRB could be elevated to 1.28 × 10^9 t, within which the Grain for Green Project in the Lüliang Mountains contributed to a slight 0.9% increase in CS (1.29 × 10^9 t), although this was partially offset by mining area development. The SDYRB, by leveraging a "CL-wetland" system (with a wetland carbon density of 2.31 × 10^4 t/km²), curtailed the declining trend and reversed carbon loss. Should urban expansion be allowed to proceed unchecked under the NDS, the three provincial sections would incur a high carbon cost (Fig. 11).

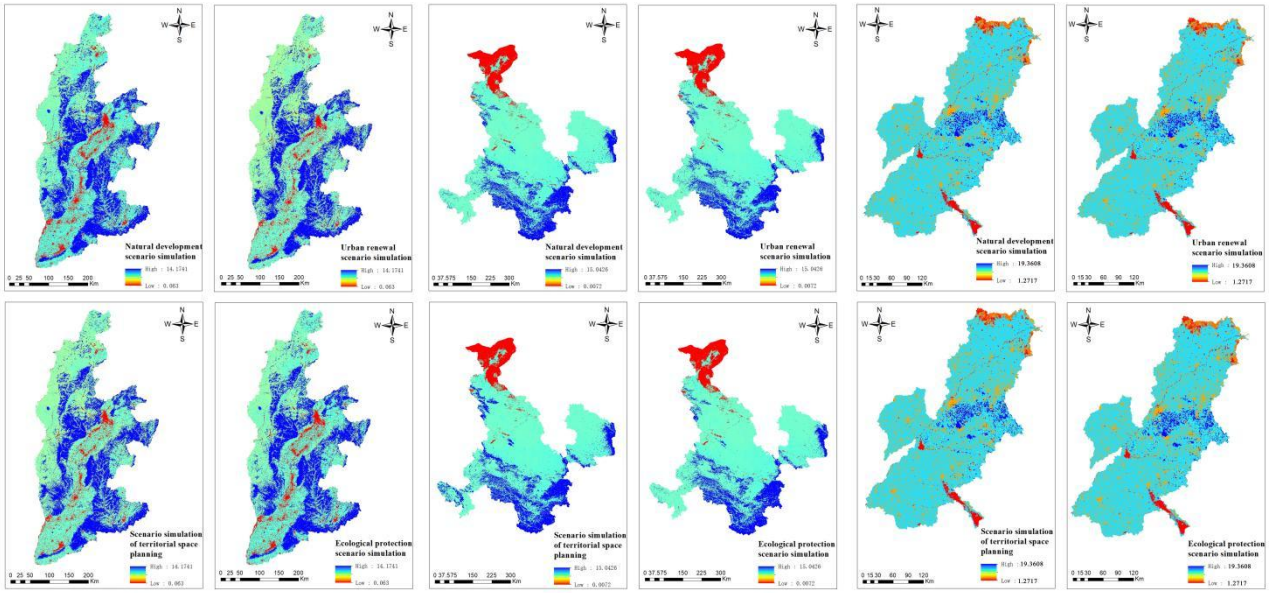


Fig. 11 Projected CS under different scenarios for the SYRB, GYRB, and SDYRB in 2035

4. Discussion

4.1 Differences in Driving Mechanisms

Taking SYRB, GYRB, and SDYRB of the YRB as the study areas, this study couples the PLUS-InVEST model with dynamic carbon density correction techniques to systematically analyze the impact of land use change on CS from 2005 to the present, and to project the evolutionary trends of CS under multiple scenarios in 2035. Four development modes—the NDS, UORS, TSPS, and EPS [33]—were established. For the first time, a systematic comparison was conducted by linking the Shanxi, Gansu, and Shandong provincial sections across the upper, middle, and lower reaches of the Yellow River. The core driving factors underlying the regional differences in CS were revealed from three dimensions: historical evolution, future responses, and spatial differentiation. The results indicate that the growth of CS in the SYRB is highly dependent on the intensity of ecological conservation policy implementation; the fluctuation of CS in the GYRB is jointly determined by territorial spatial control and the process of ecological restoration; and the change in CS in the SDYRB is dominated by the structural contradiction between urban expansion and agricultural intensification.

The patterns of land use transition, the spatiotemporal differentiation characteristics of CS, and the driving mechanisms revealed in this study are generally consistent with the research conclusions of Yang et al. [34] for the entire YRB and typical sections. However, influenced by the heterogeneity of regional natural endowments, economic development levels, and policy orientations, the CS exhibits pronounced spatial differentiation characteristics. A comparative interpretation by region is provided below.

4.1.1 Natural Factors (Precipitation Reduction) and Socio-economic Factors (Overgrazing) Jointly Contributed to CS

Fluctuations in the GYRB

In this region, grasslands are the dominant vegetation type, rendering them particularly susceptible to climatic variability and anthropogenic pressures. The interplay between precipitation patterns and livestock grazing intensity emerges as a principal determinant of regional carbon balance. Our observations indicate a gradual upward trend in CS for the Gansu section over the study period, albeit with periodic oscillations—a pattern that mirrors the findings of Fu et al. (2024) for the broader upper Yellow River region. Existing research indicates that FL expansion and the conversion of unused land to ecological land can enhance CS in the upper reaches, whereas grassland degradation and disorderly construction land expansion can weaken the carbon sink capacity. From 2005 to 2023, through measures such as the Grain for Green Project and the ecological restoration of unused land, the areas of FL and grassland in the Gansu section continuously increased, and the CS rose from 2.35×10^9 t to 2.37×10^9 t, corroborating the rule proposed by Lv et al. [35] that "ecological restoration in the upper Yellow River promotes carbon sink growth."

This study further reveals that CS fluctuations in the Gansu section are jointly driven by precipitation reduction and overgrazing. This differs from the conclusion of Qi et al. [36], who argued that "the decline in basin-wide CS is attributable to construction land expansion and CL loss," which failed to capture the unique coupled climatic-grazing pressure characteristic of the upstream arid zone. The mean annual precipitation in the Gansu section is only 300 mm, resulting in low grassland carrying capacity. Overgrazing has led to grassland degradation over an area of 2,560 km^2, corresponding to a carbon loss of 1.33×10^7 t, forming a transmission chain of "climatic aridity – grassland degradation – CS decline."

Scenario simulation results indicate that the CS of the Gansu section is higher under the TSPS than under the single EPS. Although most studies consider the EPS to be most conducive to carbon sink enhancement, the high proportion of unused land and strong water resource constraints in the Gansu section mean that ecological protection alone cannot achieve sustained carbon sink growth. It is necessary to rely on territorial spatial planning to coordinate measures such as unused land conversion, grassland grazing suspension, and ecological migration to guarantee a stable increase in CS. This suggests that carbon sink enhancement in arid zones must follow a governance logic of "planning-based guidance, zoning-based control, and category-specific policy implementation," rather than a single ecological protection pathway.

4.1.2 SYRB: Policy-driven (Grain for Green Project) Dominance in Carbon Sink Increase, Offset Partially by Energy Development

From 2005 to 2023, the regional CS exhibited an overall fluctuating upward trend, reaching 1.28×10^9 t. This is consistent with the findings of Ji et al. (2025) that "CS in the Beijing-Tianjin-Hebei region is subject to the dual impacts of ecological policies and energy development" and aligns with the discovery by Ma et al. (2026) that "CS growth in the middle Yellow River is highly correlated with the intensity of Grain for Green policies."

SYRB has continuously promoted ecological projects since 2000, including the Grain for Green Project and the Beijing-Tianjin Sandstorm Source Control Project. From 2005 to 2023, the net increase in FL area reached 1.2×10^4 km^2, directly contributing to a cumulative CS increase of 0.09×10^9 t, with a contribution rate of 72.3%, corroborating the viewpoint of Wang et al. (2025) that "ecological conservation policies are the core driving force for carbon sink enhancement in the middle reaches." However, it is noteworthy that energy activities in the Shanxi section, such as coal mining and thermal power development, have caused land degradation and vegetation destruction. From 2005 to 2023, the carbon loss resulting from the expansion of industrial and mining land amounted to 0.03×10^9 t, offsetting approximately 33% of the ecological carbon sink benefits. This mechanism aligns with the conclusion of Cai et al [37] that "the ecological benefits in energy-dependent regions are easily offset by resource exploitation."

Under EPS, SYRB CS reached 1.26×10^9 t, but the highest values were attained under UORS (1.28×10^9 t) and TSPS (1.28×10^9 t), highlighting the importance of coordinated urban renewal and spatial planning rather than relying solely on ecological protection. This is consistent with the understanding of Alam et al. (2012) that "the carbon sink enhancement effect of ecological engineering must avoid disturbance from high-intensity human activities" and provides a scientific basis for the "synergistic development of ecological conservation and green growth" in energy-

dependent regions of the middle Yellow River.

4.1.3 SDYRB: Prominent Contradiction between Urbanization and Agricultural Intensification, Requiring a Balance between Food Security and Ecological Conservation

From 2005 to 2023, its CS declined continuously, consistent with the findings of Yang et al. (2022) and Niu et al. [38] on the decreasing trend in CS in the lower Yellow River. Yang et al. (2022) attributed this decline to the rapid expansion of construction land and the encroachment upon CL and FL in the lower reaches; Niu et al. (2024) further pointed out that wetland shrinkage and the diminishment of CL carbon pools have exacerbated the loss of carbon sinks. This study reveals that in the Shandong section, construction land expanded by 46.28%, CL loss amounted to 5,172.49 km^2, and CS decreased from 1.04×10^9 t to 0.99×10^9 t, a reduction of 4.55%, which is entirely consistent with the aforementioned driving mechanisms.

This study finds that the CS in the Shandong section varies moderately across the four scenarios, with TSPS yielding the highest value (0.99×10^9 t) and EPS the lowest (0.94×10^9 t), a difference of approximately 4.8%. This study finds that the CS in the Shandong section exhibits very limited fluctuation across the four scenarios, which aligns with the conclusion of Wu et al. (2024) that the CS in the lower reaches has low sensitivity to policy scenarios, but is contrary to the conclusions drawn for most ecologically dominant regions. Wu et al. (2024) argued that the strict CL redline in the lower Yellow River, coupled with stable CL and wetland carbon pools, results in modest changes in total CS, with inter-scenario differences in total CS generally remaining below 0.05%. As a major grain-producing area and an economically developed region, the Shandong section is subject to strong rigid constraints on CL conservation. The focus of CS regulation is not on increasing the total amount but on balancing food security, urbanization, and ecological conservation—enhancing soil carbon sinks by improving the composite "cultivated land-wetland" system rather than expanding FL area.

Therefore, the primary contradiction in enhancing CS in the Shandong section does not lie in the regulation of the total carbon quantity. Under the premise of safeguarding the CL redline, the goal is to achieve an optimized land use structure and the healthy enhancement of the soil carbon pool through precise wetland conservation, improved agricultural management, and the refinement of the ecological compensation mechanism, thereby attaining the unified objectives of food security, ecological conservation, and low-carbon development.

4.2 Conservation of the Entire YRB

This study innovatively integrates the Shanxi, Gansu, and Shandong provincial sections across the upper, middle, and lower reaches of the Yellow River, conducting a systematic comparative analysis that effectively overcomes the limitations of previous studies, which were largely confined to individual provinces or broad, generalized analyses of the entire basin. Specifically, the study by Yang et al. (2022) indicated that CS in the YRB exhibited an overall decline from 2005 to 2018, and that even under the Natural Development and EPS for 2030, CS remained at risk of continued decline. The calculation results of Qi et al. (2024) indicated that the CS of the terrestrial ecosystem in the YRB exhibited phased increases, with high-value CS clusters primarily concentrated in the mountainous and hilly areas of the upper and middle reaches. Through various research methods, including sub-sectional mechanism analysis and multi-scenario simulation projections, this study clarifies the differentiated ecological management pathways for the upper, middle, and lower reaches of the Yellow River, providing refined scientific support for basin-wide ecological conservation and the enhancement of carbon sink quality in the YRB.

The Gansu section strictly adheres to the control logic of the TSPS, centered on climate-adaptive governance and the sustainable utilization of grassland resources, and implements a management model of grazing suspension to promote greening, whereby grazing intensity is strictly controlled within the threshold of grassland ecological carrying capacity. This management approach mutually corroborates the conclusion proposed by Li et al. [39] that "the ecological conversion of unused land to grassland is the core pathway for CS growth in the upper reaches." Based on the regulatory rules of the TSPS, this study increases the probability of ecological conversion from unused land to CL, FL, and grassland by 20%, promotes drought-tolerant native shrub vegetation such as Caragana korshinskii and

Hippophae rhamnoides in the arid areas of central Gansu, and concurrently implements ecological restoration of degraded land and saline-alkali land, effectively elevating the CS level in low-carbon-density areas, which is highly consistent with the carbon sink enhancement pathway through upstream ecological restoration proposed by Lv et al. (34 2025).

The Shanxi section, guided by the TSPS, establishes a dual-wheel governance model of "intensive Grain for Green Project implementation + rigid control of new energy land use," organically integrating mining area ecological restoration, coal production capacity phase-out, and the spatial layout of new energy industries. Within the ecological redline control areas of the Lüliang Mountains and Taihang Mountains, mandatory Grain for Green Project implementation is enforced on sloping CL with gradients exceeding 25°. Leveraging the constraints of territorial spatial planning, reclaimed mining land is prioritized for the layout of new energy projects such as photovoltaic and wind power, and an ecological benefit-loss assessment system for energy development is established, thereby achieving the synergistic advancement of permanent basic CL conservation and mining area ecological restoration. This concept of coordinated development and conservation governance is consistent with the collaborative governance logic for the Beijing-Tianjin-Hebei regional ecological space proposed by Ji et al. (2025), and also highly compatible with the ecological control requirements for energy-dependent basins in the middle reaches proposed.

The Shandong section strictly upholds the redline of CL conservation, and through spatial structure optimization and agricultural technological innovation, constructs a composite cultivated land-wetland carbon sink system. Taking the UORS as the entry point, it promotes greening and quality improvement within urban areas, implements the wetland-oriented transformation of canal and drainage systems in the Yellow River Delta region, establishes a cross-city horizontal ecological compensation mechanism between Jinan and Dongying, explores market-based trading pathways for ecological carbon sinks from saline-alkali land, and promotes the transition of coastal unused land into constructed wetland carbon pools. This development pathway comprehensively balances the three major objectives of food security, urban expansion, and ecological conservation, aligning with the research concept proposed by Luo et al. [40] on enhancing vegetation carbon sink efficiency in the YRB, and mutually corroborating the research conclusions of Niu et al. (2024) on the priority conservation of downstream wetland carbon pools.

At the cross-provincial synergistic level, Shanxi, Gansu, and Shandong jointly establish an SGS Corridor CS dynamic monitoring platform. Leveraging remote sensing technology, a basin-wide intelligent monitoring network for the YRB is constructed to track key processes such as grassland degradation control in Gansu, mining area ecological restoration in Shanxi, and CL conversion in Shandong in real time. This builds a chain-like spatial governance system of "upper reach ecological restoration – middle reach CL quality improvement – lower reach urban synergy," realizes cross-regional linked control of the "Three Zones and Three Lines," and forms a paradigm of differentiated control and integrated carbon sink enhancement across the upper, middle, and lower reaches, thereby providing a replicable and scalable cross-regional synergistic governance solution for ecological conservation and high-quality development in the YRB.

4.3 Model Uncertainty

A primary source of uncertainty in our simulation of CS for the SGS Corridor stems from the inherent spatial variability of carbon density parameters [41]. The three provinces under investigation, Shanxi, Gansu, and Shandong, exhibit considerable divergence in their natural environmental baselines and land management histories. This heterogeneity leads to significant spatial gradients in carbon density, which inevitably introduces a degree of imprecision into our model outputs.

This study employs the coupled PLUS-InVEST model framework, which is consistent with the methodological systems adopted by scholars in mainstream basin-scale CS research; therefore, the sources of model uncertainty also share homologous characteristics. In the process of carbon density parameter assignment, most existing related studies mitigate parameter errors arising from differences in soil and vegetation types through methods such as meteorological

correction or regional mean smoothing; however, these approaches still cannot entirely eliminate the bias induced by spatial heterogeneity, and this limitation also exists in the present study. Regarding the selection of driving factors and scenario setting, although the PLUS model has incorporated three categories of fundamental driving factors—namely, the natural environment, socio-economic conditions, and land use policies—the characterization of dynamic anthropogenic policies, such as energy regulatory policies, ecological compensation mechanisms, and detailed grazing control regulations, remains insufficiently refined. Concurrently, the scenario schemes established in this study are based on territorial spatial planning objectives, which deviate to some extent from the spontaneous evolution processes of land use in reality. This inadequacy aligns with the issue of "insufficiently refined characterization of policy-driven factors" noted by Fu et al (2024). Furthermore, the InVEST model by default assigns homogeneous carbon density values to the same land use type, and therefore cannot fully reflect the dynamic changes in carbon pools induced by factors such as vegetation growth succession stages, CL cultivation measures, and grazing intensity fluctuations. This also represents a common deficiency in most current model application studies within this field.

To further improve the accuracy of future CS simulations, subsequent research may rely on machine learning methods to construct a refined spatial model of carbon density at a 1 km grid resolution, optimizing parameter thresholds by integrating field sampling data and long-term in-situ monitoring data. Simultaneously, dynamic policy variables should be incorporated into the model, and multi-gradient development scenarios should be established for comparative simulation, thereby further enhancing the practical guidance value of the simulation outcomes. By improving model algorithms and integrating multi-source remote sensing and ground-based monitoring data, more precise decision support can be provided for land use optimization and carbon sink enhancement in the YRB.

5. Conclusion

(1) From 2005 to 2023, SYRB and GYRB experienced CS increases of 0.85% and 0.91%, respectively, driven primarily by grassland and FL expansion, whereas SDYRB declined by 4.55% due to rapid construction land expansion.

(2) Multi-scenario projections for 2035 show that TSPS yields the highest CS in GYRB (2.38×10^9 t) and SDYRB (0.99×10^9 t), while in SYRB, UORS and TSPS both reach 1.28×10^9 t; EPS consistently performs worse across all three sections. Thus, differentiated policies are imperative: Shanxi should combine urban renewal with spatial planning, Gansu must rely on TSPS-driven unused land restoration and grazing control, and Shandong needs strict TSPS to limit construction land sprawl and CL conversion.

(3) Driving mechanisms differ markedly: SYRB's ecological gains from Grain for Green were partially offset by energy development; GYRB's fluctuations were driven by declining precipitation and overgrazing; SDYRB's carbon loss was dominated by urban–agricultural intensification conflicts. Differentiated "Three Zones and Three Lines" control is recommended to synergistically enhance basin-wide carbon sink function.

Consent to Publish Declarations

This manuscript has not been published or presented elsewhere in part or in entirety and is not under consideration by another journal. We have read and understood your journal's policies, and we believe that neither the manuscript nor the study violates any of these. There are no conflicts of interest to declare. All of the authors agree to submit a research article for publication in Carbon Balance and Management. Thanks.

Availability of data and materials

The datasets used and/or analysed during the current study available from the corresponding author on reasonable request.

Competing interests

The authors declare that they have no conflict of interest.

Ethics and Consent to Participate declarations: not applicable.

Funding

This work was supported by:

Shanxi Agricultural University Science and Technology Innovation Promotion Project, CXGC2025085;

Planning Project for Philosophy and Social Sciences In Shanxi Province, 2024QN045;

Shanxi Agricultural University Science and Technology Innovation Promotion Project, CXGC2026003.

Authors' contributions

Ruyang Xi: Data curation, Investigation, Methodology, Writing - original draft, Writing - review & editing. **Ruiying Li:** Data curation, Writing - original draft. **Jingxuan Wu:** Data curation. **Fanyu Yue:** Data curation, Investigation. **Jiakai Ma:** Investigation. **Zhilei Zhen:** Data curation, Methodology. **Ben Wang:** Data curation, Funding acquisition, Conceptualization, Writing- review & editing.

References

1.Du, L., Dong, C., Kang, X., Gu, L., Qian, X., 2023. Spatiotemporal evolution of land cover changes and landscape ecological risk assessment in the Yellow River Basin, 2015–2020. Journal of Environmental Management. 332, 117149. https://doi.org/10.1016/j.jenvman.2022.117149.

2. Fang, Z., Xue, S., Ding, T., Wang, Y., Yang, S., Huang, Z., Zhou, Q., Wang, Y., Chen, J., 2022. Impacts of land use/land cover changes on ecosystem services in ecologically fragile regions. Science of the Total Environment. 831, 154967. https://doi.org/10.1016/j.scitotenv.2022.154967.

3.Wang, P., Li, R., Liu, D., Wu, Y., 2022a. Dynamic characteristics and responses of ecosystem services under land use/land cover change scenarios in the Huangshui River Basin, China. Ecological Indicators. 144, 109539. https://doi.org/10.1016/j.ecolind.2022.109539.

4. Tang, X., Ma, K., Wang, W., He, H., Fang, J., Xie, Z., Du, S., Li, S., Han, S., Hu, H., Wang, G., Wan, H., Han, W., Zhao, Y., Ma, Y., Yan, J., He, N., Zhou, G., Wu, B., Bai, Y., Zhao, X., Yu, G., Tang, Z., Shi, X., Yang, Y., 2018. Carbon pools in China's terrestrial ecosystems: New estimates based on an intensive field survey. Proceedings of the National Academy of Sciences. 115 (16): 4021-4026. https://doi.org/10.1073/pnas.1700291115.

5.Zhou, G., Zhou, L., Ji, Y., Zhou, M., 2022. Advances in the carbon sink potential of terrestrial ecosystems in China. Chinese Science Bulletin. 67 (31): 3625-3632. https://doi.org/10.1360/tb-2022-0032.

6.Zhao, N., Zhou, L., Zhuang, J., Wang, Y., Zhou, W., Chen, J., Song, J., Ding, J., Chi, Y., 2021. Integration analysis of the carbon sources and sinks in terrestrial ecosystems, China. Acta Ecologica Sinica. 41 (19):7648-7658. https://doi.org/10.5846/stxb202004271012.

7.Cheng, H., Huang, Y., Hu, Y., Zhang, X., He, J., Jiang, W., 2026. Land-use-associated carbon storage variation in the Dashanbao Alpine wetland region: An InVEST-based assessment with soil profile interpretation. Ecological Indicators. 189, 115150. https://doi.org/10.1016/j.ecolind.2026.115150.

8.Song, H., Zhang, X., Xiao, H., Hu, T., Xu, B., 2026. Linking land cover changes to carbon storage in Hunan Province, China: Insights from multi-task learning. Journal of Cleaner Production. 570, 148770. https://doi.org/10.1016/j.jclepro.2026.148770.

9.Li, F., Xu, X., Huang, X., Du, J., 2026. Spatio-temporal differentiation and influencing factors of coupling coordination degree in the economy-ecology-green finance system across nine provinces (regions) of the Yellow River Basin. Ecological Indicators. 187, 114978. https://doi.org/10.1016/j.ecolind.2026.114978.

10.Wang, H., Zhang, C., Xu, H., Hong, X., Wang, C., Niu, J., 2024a. Spatial heterogeneity evolution and driving mechanism analysis of land use change in major river basins: a case study of urban agglomerations in the Yellow River Basin. Geocarto International. 39 (1). https://doi.org/10.1080/10106049.2024.2418453.
11.Wang, J., Li, Q., Liu, X., Li, Y., Li, L., Wang, S., 2022b. The Spatiotemporal Evolution and Prediction of Carbon Storage in the Yellow River Basin Based on the Major Function-Oriented Zone Planning. Sustainability. 14 (13): 7963. https://doi.org/10.3390/su14137963.
12.Xu, C., Ai, M., Zhao, J., Wang, F., Wang, J., Zhang, Q. B., Yu, Q., Qiu, S., 2023. Effects of land use/cover change on carbon storage between 2000 and 2040 in the Yellow River Basin, China. Ecological Indicators. 151: 110345. https://doi.org/10.1016/j.ecolind.2023.110345.
13.Ma, J.-K., Zhen, Z., Hao, Z., Shen, Y., 2025. Spatial-temporal evolution of carbon storage and its driving factors in the Shanxi section of the Yellow River Basin, China. Ecological Modelling. 502: 111039. https://doi.org/10.1016/j.ecolmodel.2025.111039.
14.Wang, H., Jin, Y., Zhang, B., Yue, Y., Wu, L., 2024b. Impacts of climate and land use change on terrestrial carbon storage: A multi-scenario case study in the Yellow River Basin (1992–2050). Science of the Total Environment. 930: 172557. https://doi.org/10.1016/j.scitotenv.2024.172557.
15.Wang, Z., Wang, Q., Zhao, L., Zhao, X., Qin, P., Feng, C., 2022c. Ecological protection and restoration strategies in the Yellow River Basin (Shandong Section). CRC Press eBooks. 10-19. https://doi.org/10.1201/9781003363545-2.
16.Zhang, T., 2023a. Temporal and Spatial Evolution of Land Use in Gansu Section of The Yellow River Basin and Analysis of Driving Forces. Academic Journal of Science and Technology. 4 (3). https://doi.org/10.54097/ajst.v4i3.4901.
17.Fu, K., Jia, G., Yu, X., Chen, L., 2024. How has carbon storage changed in the Yili-Tianshan region over the past three decades and into the future? What has driven it to change? Science of the Total Environment. 945: 174005. https://doi.org/10.1016/j.scitotenv.2024.174005.
18.Zhang, Y., Sun, D., Liao, X., 2024a. A Coupled InVEST-PLUS Model for the Spatiotemporal Evolution of Ecosystem Carbon Storage and Multi-Scenario Prediction Analysis. Land. 13 (4): 509. https://doi.org/10.3390/land13040509.
19.Li, X., Peterson, J., Liu, G.-J., Qian, L., 2001. Assessing regional sustainability: the case of land use and land cover change in the middle Yiluo catchment of the Yellow River basin, China. Applied Geography. 21 (1), 87–106. https://doi.org/10.1016/S0143-6228(00)00020-5.
20.Shi, H., Duan, H., Li, X., Wang, G., Chen, A., Liang, D., 2026. Impact of land use change on carbon storage based on the PLUS–InVEST model: A case study in the urban belt along the Yellow River, China. Journal of Arid Land. 18 (3), 452–476. https://doi.org/10.1016/j.jaridl.2026.03.006.
21.Lu, C., Jia, K., Zheng, Z., Xiao, Q., 2022. PLUS-Model Based Multi-Scenario Land Space Simulation of the Lower Yellow River Region and Its Ecological Effects. Sustainability. 14 (11): 6942. https://doi.org/10.3390/su14116942.
22.Henzler, J., Beyer, N., Hanß, S., Fiedler, S., Simpkins, C. E., Wiegand, K., 2026. Coupling agent-based and InVEST® models for spatio-temporal simulation of land-use change effects on ecosystem services. Environmental Modelling & Software. 204, 107095. https://doi.org/10.1016/j.envsoft.2026.107095.
23.Ma, Y., Wang, J., Xin, P., Zhao, Z., Zhang, X., Yang, Y., Gao, T., Qiu, L., 2026. Assessing carbon storage dynamics and policy impacts: Application of InVEST-PLUS framework in the Qinling Mountains, China. Land Use Policy. 164, 107947. https://doi.org/10.1016/j.landusepol.2026.107947.
24.Wu, Q., Li, W., Wang, T., Du, P., Ruan, Z., 2024. Spatial–temporal evolution analysis of multi-scenario land use and carbon storage based on PLUS-InVEST model: A case study in Dalian, China. Ecological Indicators. 166:112448. https://doi.org/10.1016/j.ecolind.2024.112448.
25.Ji, W., Yang, F., Feng, Z., Zhang, H., Zhang, B., Lv, H., Wang, Z., Yu, Z., Li, H., He, M., 2025. Carbon

storage change, driving mechanism, and scenario prediction in Beijing-Tianjin-Hebei region for regional carbon neutral target: From history to future. The Science of the total environment. 993: 180028. https://doi.org/10.1016/j.scitotenv.2025.180028.

26.Alam, S. A., Starr, M., Clark, B., 2012. Tree biomass and soil organic carbon densities across the Sudanese woodland savannah: A regional carbon sequestration study. Journal of Arid Environments. 89. https://doi.org/10.1016/j.jaridenv.2012.10.002.

27.Pascual, A., Giardina, C. P., Selmants, P. C., Laramee, L. J., Asner, G. P., 2021. A new remote sensing-based carbon sequestration potential index (CSPI): A tool to support land carbon management. Forest Ecology and Management. 494, 119343. https://doi.org/10.1016/j.foreco.2021.119343.

28.Chen, G. S., Yang, Y. S., Liu, L. Z., Li, X. B., Zhao, Y. C., Yuan, Y. D., 2007. Research review on total belowground carbon allocation in forest ecosystems. Journal of Subtropical Resources and Environment. 2(1), 34–42. https://doi.org/10.19687/j.cnki.1673-7105.2007.01.005.

29.Zhang, C., Liu, Y., Gao, Y., Zheng, Z., Li, K., Jia, Q., 2024b. Evaluation and multi scenario simulation of ecosystem service value in Zhengzhou Metropolitan Area based on PLUS model. Measurement Sensors. 32: 101079. https://doi.org/10.1016/j.measen.2024.101079.

30.Zhang, J., Wang, J., Huang, S., Chen, Y., Liang, B., 2023b. Spatiotemporal variation and prediction of NPP in Beijing-Tianjin- Hebei region by coupling PLUS and CASA models. Ecological Informatics. 81: 102620. https://doi.org/10.1016/j.ecoinf.2024.102620.

31.Qu, S., Li, L., Han, L., 2025. Regional Responses of Ecosystem Service Security to Land Use Changes and Driving Mechanisms: Insights from Nearly 40 Years of Observations in Shaanxi, China. Journal of Environmental Chemical Engineering, 13,(3), 116224. https://doi.org/10.1016/j.jece.2025.116224.

32.Wang, C., Zhao, X., Zhao, H., Zheng, H., Yu, E., Wang, C., Zhang, Z., He, J., Li, Y., 2025. Driving factors of ecosystem services and their trade-offs and synergies in different land use functional zones: A case study of Shanxi Province, China. Environmental and Sustainability Indicators. 2025: 101011. https://doi.org/10.1016/j.indic.2025.101011.

33.Zhang, J., Cao, P., Roosli, R., 2025. Assessing land use and carbon storage changes using PLUS and InVEST models: A multi-scenario simulation in Hohhot. Environmental and Sustainability Indicators, 26, 100655. https://doi.org/10.1016/j.indic.2025.100655.

34.Yang, R., Chen, S., Ye, Y., Chen, H., 2022. Spatiotemporal evolution and prediction of land use/land cover changes and ecosystem service variation in the Yellow River Basin, China. Ecological Indicators. 145: 109579. https://doi.org/10.1016/j.ecolind.2022.109579.

35.Lv, Q., Zhang, W., Wang, C., Liu, W., Fan, H., Yang, H., Feng, G., Huang, X., Qin, Y., Qiao, Y., Wang, J., Cui, L., Han, Y., Wang, W., Zhang, Y., Yao, Y., 2025. Estimating Regional Terrestrial Ecosystem Carbon Sinks on Multi-Model Coupling Approach. Ecological Indicators, 178, 114041. https://doi.org/10.2139/ssrn.5204292.

36.Qi, S., Zhang, H., Zhang, M., 2024. Evolutionary characteristics of carbon sources/sinks in Chinese terrestrial ecosystems regarding to temporal effects and geographical partitioning. Ecological Indicators. 160: 111923. https://doi.org/10.1016/j.ecolind.2024.111923.

37.Cai, C., Fan, M., Yao, J., Zhou, L., Wang, Y., Liang, X., Liu, Z., Chen, S., 2023. Spatial-temporal characteristics of carbon emissions corrected by socio-economic driving factors under land use changes in Sichuan Province, southwestern China. Ecological Informatics. 77. https://doi.org/10.1016/j.ecoinf.2023.102164.

38.Niu, H., Chen, S., Xiao, D., 2024. Multi-Scenario land cover changes and carbon emissions prediction for peak carbon emissions in the Yellow River Basin, China. Ecological Indicators. 168. https://doi.org/10.1016/j.ecolind.2024.112794.

39.Li, H., Zhang, K., Liu, Y., Qin, Y., Wang, W., Wang, M., Liu, Y., Li, Y., 2025. Spatiotemporal evolution of

673 land use and carbon storage in China: Multi-Scenario simulation and driving factor analysis based on the
674 PLUS-InVEST model and SHAP. Environmental Research. 279, 121860.
675 https://doi.org/10.1016/j.envres.2025.121860.
676 40.Luo, L., Wang, Y., Zhang, X., Liu, Y., Fang, X., 2022. Where is the pathway to sustainable urban
677 development? Coupling coordination evaluation and configuration analysis between low-carbon development
678 and eco-environment: A case study of the Yellow River Basin, China. Ecological Indicators. 144:109473.
679 https://doi.org/10.1016/j.ecolind.2022.109473.
680 41.Nelson, E., Kareiva, P., Naidoo, R., Tallis, H., Regetz, J., Ricketts, T. H., Cameron, D., Daily, G. C., Shaw, M.
681 R., Mendoza, G., Lonsdorf, E. V., Chan, K. M. A., Polasky, S., Goldstein, J., 2009. Modeling multiple
682 ecosystem services, biodiversity conservation, commodity production, and tradeoffs at landscape scales.
683 Frontiers in Ecology and the Environment. 7 (1): 4-11. https://doi.org/10.1890/080023.